J. Bangladesh Acad. Sci. 46(2); 175-183: December 2022 DOI: 10.3329/jbas.v46i2.63416

Journal of Bangladesh Academy of Sciences

Journal homepage: http://www.bas.org.bd/publications/jbas.html

Research Article

Estimation of prolonged lifetimes of excited states of neutral oxygen atom (OI) by time-resolved laser-induced breakdown spectroscopy (TR-LIBS)

Abul Fazal Mohammed Yusuf Haider[1,3], Nabil Md Rakinul Hoque[2], Arifur Rahaman and Zulfiqar Hasan Khan[*]

Department of Physics, University of Dhaka, Dhaka, Bangladesh

RTICLE INFO

Article History

Received: 28 November 2022
Revised: 13 December 2022
Accepted: 15 December 2022

Keywords: Words: LIBS, Upper state, Lifetime, Self-absorption, Radiation trapping

ABSTRACT

Lifetimes of the upper states of excited oxygen atoms corresponding to transitions to the common lower state in the case of the emission lines around 777 nm and 844 nm have been estimated by measuring the line intensities as a function of the delay time between the Q-switching of the laser and the opening of the window of the ICCD. In the case of the emission line around 777 nm, resulting from the transitions from the three very closely spaced upper energy levels, $2s^2\ 2p^3\ (^4S^0)\ 3p\ ^5\mathbf{P_3}$ (777.194 nm), $2s^2\ 2p^3\ (^4S^0)\ 3p\ ^5\mathbf{P_2}$ (777.417 nm) and $2s^2\ 2p^3\ (^4S^0)\ 3p\ ^5\mathbf{P_1}$ (777.539 nm) to the common lower energy level $2s^2\ 2p^3\ (^4S^0)\ 3s\ ^5\mathbf{S_2}$, the lifetime was measured to be 253 ns. Similarly, in the case of the emission-line around 844 nm, resulting from the transitions from the three very closely spaced upper energy levels $2s^2\ 2p^3\ (^4S^0)\ 3p\ ^3\mathbf{P_0}$ (844.625 nm), $2s^2\ 2p^3\ (^4S^0)\ 3p\ ^3\mathbf{P_2}$ (844.636 nm) and $2s^2\ 2p^3\ (^4S^0)\ 3p\ ^3\mathbf{P}_1$ (844.676 nm) to the common lower energy level $2p^3\ (^4S^0)\ 3s\ ^3\mathbf{S_1}$, the lifetime was measured to be 278 ns by this technique. The measured lifetimes in our experiment, for both 777 nm and 844 nm atomic transition lines of oxygen (O), are almost nine times higher than the theoretical value. Self-absorption and radiation trapping are possible mechanisms responsible for the mismatch between measured and intrinsic lifetimes. Last but not least, utilizing the TR-LIBS technique is yet another incredible application to estimate the prolonged lifetime of closely spaced excited states of an atom in the presence of self-absorption and radiation trapping. The average plasma cooling temperature (excitation temperature) lifetime was found to be 1183 ns, which is compatible with the previously reported values.

Introduction

Laser-Induced Breakdown Spectroscopy (LIBS) is a convenient, competent, and fast elemental analysis technique. LIBS can be employed for plasma diagnostics (Haider and Khan, 2012; Hahn and Omenetto, 2010), such as measuring plasma's electron density and temperature by the Saha-Boltzmann plot (Shaikh et al., 2006; Quintero et al. 1997; Aguilera and Aragón 2007). Another novel application of LIBS is the measurement of lifetimes of atomic and ionic states (Haider et al. 2014).

The lifetime of upper states must be taken into account when studying light propagation in atomic line filters (Molisch and Oehry 1998), discharge lamps (Rajaraman and Kushner 2004; Camparo and MacKay 2007), trapped cold atoms (Hillenbrand et al., 1995; Balik et al., 2009), stellar media (Boldyrev and Gwinn 2003), or Laser media (Zhang et al., 2017). In optical applications like scintillators, amplifiers, and display systems, the lifetime is a crucial spectroscopic parameter (Stoita et al., 2010). Lifetime measurements are needed in areas such as astrophysical abundance determinations and plasma diagnostics (Curtis 1976). Lifetimes of different atomic/ionic transitions were estimated using time-resolved laser-induced fluorescence (TR-LIF) (Xu et al., 2004; Mayo et al.,

[*]Corresponding author: <zulfiqarshuvo@du.ac.,bd>

[2]*Biomedical Engineering Department, Washington University, St Louis, USA*

[3]*Department of Mathematics and Natural Sciences, BRAC University, Dhaka, Bangladesh*

2005; Mayo et al., 2006), LIF (Hannaford and Lowe 1983; O'Brian and Lawler 1992), and beam-foil (Pinnington et al., 1988; Berry et al., 1971) technique, high-frequency deflection method (O'Brian and Lawler 1992), and delayed coincidence methods (Smith et al., 1975; King and Adams 1974). The comparison of various techniques demonstrates that no single procedure can be employed to calculate lifetimes for all types of states in atoms, ions, and molecules over a wide spectral region and lifetime. For example, the beam-foil technique of measuring lifetimes is only restricted to the atoms, whereas the high-frequency deflection method can measure the lifetime of ions. In contrast, time-resolved LIBS (TR-LIBS) can be employed for lifetime measurement for different transitions regardless of wavelength and atomic/ionic/molecular states.

In our previous work, LIBS coupled with time-resolved gated ICCD was employed to measure the lifetimes of some excited states of the Nitrogen atom (Haider et al., 2014). In this paper, we extend the same technique to measure the lifetime of excited states of the oxygen atom. The estimated lifetime is 253 ns and 278 ns for the emission lines around wavelengths of 777 nm and 844 nm, respectively, which is about nine times higher than the corresponding theoretical value. This augmented lifetime of oxygen atoms is likely linked with (i) self-absorption of oxygen atoms as the upper states involved are very close together in energy and (ii) radiation trapping.

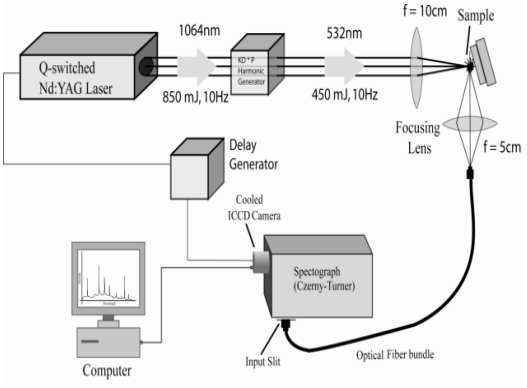

Fig. 1. Schematic diagram of TR-LIBS to find the lifetime of excited states.

Experimental setup

For performing the LIBS experiment, a Q-switched Nd: YAG laser of model Spectra-Physics LAB-170-10 (Figure 1) was focused having the following parameters: wavelength of 532 nm with a pulse duration of 8 ns; and a repetition rate of 10 Hz with a maximum pulse energy of 450 mJ. Additionally, it contained harmonic generators that used KDP crystals to produce the fundamental up to the fourth harmonic. The actual energy of the pulse employed was 40 mJ. Having divergence, Θ<0.5 mrad, the beam maintains a Gaussian shape in the far-field (Haider and Khan, 2012).

The output at 532 nm, i.e., the second harmonic of laser, was used and focused onto the air of the laboratory at room temperature using a convex lens of about 10 cm focal length. Therefore, intense, brief, and weakly ionized plasma is produced, and the resulting emitted radiation is focused by a fused quartz lens (aperture 50 mm) onto multimode silica fiber (length 3 m). The electric field intensity at the focus of the laser beam (about 200 microns in diameter) is sufficient to accelerate the electrons produced by primary ionization. In turn, they produce secondary and tertiary ionization. Thus, a weakly ionized plasma is created via laser ablation where the percentage of electrons is <10% of other species present in the plasma. (Haider et al., 2014).

The optical fiber's output was attached to the slit present at the entrance of a spectrograph in the Czerny-Turner configuration with a 75 cm focal length (Acton Model SP-2758). To provide high- and low-resolution spectra in the wavelength range of 190-880 nm, the spectrograph is fitted with three interchangeable gratings with three different groves (2400, 600, and 300 grooves/mm). A spectrum with a width of about 38 nm and 9 nm can be recorded using a grating with 600 grooves and 2400 grooves per millimeter that are blazed at 500 nm and 240 nm, respectively.

The spectrograph was connected to an intensified CCD (ICCD) camera (Princeton PI-MAX), where a programmable delay generator makes the gating of the spectrograph feasible. The 1024 x 1024 pixel ICCD camera was cooled using Peltier cooling to -20 C to lower noise. The Nd: YAG laser pulse electrically activated the ICCD camera after a programmable time delay. In the current investigations, to measure emission line intensities at different delay times (200 ns-6500 ns), a gate width (t_w) of 50 μs was used. To improve the signal-to-noise ratio, average spectra are recorded from about 40 laser pulses. For each delay time t, three of these averages were used to calculate the line intensity. The manufacturer's software (Win Spec/32) was utilized to operate the Acton spectrograph and gated ICCD camera (Haider and Khan 2012).

Theory

Suppose the number of the excited atom at time t = 0 is N_1^0. Then the number of the excited atoms at time t is

$$N_1(t) = N_1^0 e^{-t/\tau} \quad (1)$$

where τ is the lifetime of spontaneous emission.

For a particular transition, the area under the emission spectrum (I) is proportional to the photon numbers emitted in the interval between t and ∞.

$$I \propto \int_t^\infty N_1(t)\, dt$$

$$\text{or, } I = \mathrm{C} \int_t^\infty N_1(t)\, dt$$

$$\text{or, } I = CN_1^0 \int_t^\infty e^{-t/\tau}\, dt \text{ ; [Using equation (1)]}$$

$$= CN_1^0\, \tau\, e^{-t/\tau}$$

$$= \mathrm{K} e^{-t/\tau}$$

$$\text{or, } \ln \mathrm{I} = \ln \mathrm{K} - \frac{t}{\tau} \quad (2)$$

where C and K both are the proportionality constants and are related as $\mathrm{K} = \mathrm{C}\, \mathrm{N}_1^0\, \tau$

Now, if one introduces a time delay t between the excitation (by laser-plasma) of the upper atomic state and the opening of the detection system (e.g., ICCD) and varies the time delay t and plot logarithm of the integrated intensity (I) as a function of this time delay t, should get a semi-logarithmic plot to estimate the lifetime of the excited state of an atom/ion corresponding to the transition to a lower state.

Again let us consider two energy levels, E_1 and E_0 (E_1 for the upper level and E_0 for the lower level). N_1 and N_0 are population densities of upper and lower levels. The Boltzmann equation gives ratios of level populations as a function of temperature,

$$\frac{N_1}{N_0} = e^{-(E_1 - E_0)/k_B T}$$

$$\text{or, } \frac{N_1}{N_0} = e^{-\Delta E/k_B T} \quad (3)$$

where k_B is the Boltzmann constant and T is the plasma temperature.

Under the local thermodynamic equilibrium (LTE) condition, and considering the plasma to be optically thin and homogeneous, the total intensity of a spectral line from an excited atom or ion is

$$\mathrm{I}\, \alpha\, \mathrm{N}_1$$

$$\text{or, } \mathrm{I} = \mathrm{Q}\mathrm{N}_1 \quad (4)$$

where Q is the proportionality constant. Now from equation (3), we can write,

$$\mathrm{I} = \frac{\mathrm{N}_0 \mathrm{Q}}{e^{\Delta E/k_B T}} \quad (5)$$

From the above equation, it can be seen that when the plasma temperature T decreases, the corresponding intensity of the emission line decreases.

Therefore, in TR- LIBS, the intensity of an emission line will reduce for two reasons, namely (1) the spontaneous decay of the excited state and (2) the cooling of the plasma.

Discussion

Lifetimes of the atomic excited states can be estimated employing time-resolved LIBS, first

reported by Haider et al. (Haider et al. 2014), where they estimated the lifetime of the neutral nitrogen atom. In this technique, the delay between the Q-switched laser pulse and the gating of the intensified CCD (ICCD) window is precisely regulated by employing a delay generator with a suitable program. Finally, the lifetimes of excited states of atomic/ionic species could be evaluated from the plot of Intensity vs. delay (Haider et al. 2014). This same approach for lifetime measurement has been incorporated to observe prolonged plasma lifetime associated with both multidimensional-plasma-grating-induced break-down spectroscopy (MIBS) (Hu et al. 2022) and plasma-grating-induced breakdown spectroscopy (GIBS) (Hu et al. 2020) compared to that of filament-induced breakdown spectroscopy (FIBS). Likewise, employing the same technique, (Yang et al. 2019) estimated the lifetime of the Si I, Ti I, Al I, and Fe I atoms in soil samples, ranging from 1.0 to 2.0 μs. Our paper, investigates the lifetime of the excited state of the neutral oxygen atom (OI) by employing well-established time-resolved LIBS. Fig. 2(a)-(c) shows how the Intensity of spectral lines of Neutral Oxygen Atom (OI) decreases as the delay increases. Fig. 3(a) represents the plot of Intensity vs. Delay time (in the range of 175 ns-6500ns) of the OI line around 777nm. The bi-exponential fit is better matched than the mono-exponential fit (Fig. 3(b)) for the data set because the bi-exponential fit (Fig. 3(c)) has a lower chi-square value (3.8108 vs. 5.5108) and a higher regression coefficient (0.9688 vs. 0.9557). A semi-logarithmic plot confirmed that the data set is indeed bi-exponential for the OI line around 777 nm (Fig 3(d)), from where exponential decay constants can be determined. However, the contribution of the slower decay process has to be deducted from the contribution of the quicker decay process to obtain the accurate value of the decay constant from the semi-log plot of InI vs. Delay. Therefore, the piecewise straight-line obtained for the relatively slow decay process was extrapolated in the 175ns-700ns delay period (Fig. 3d).

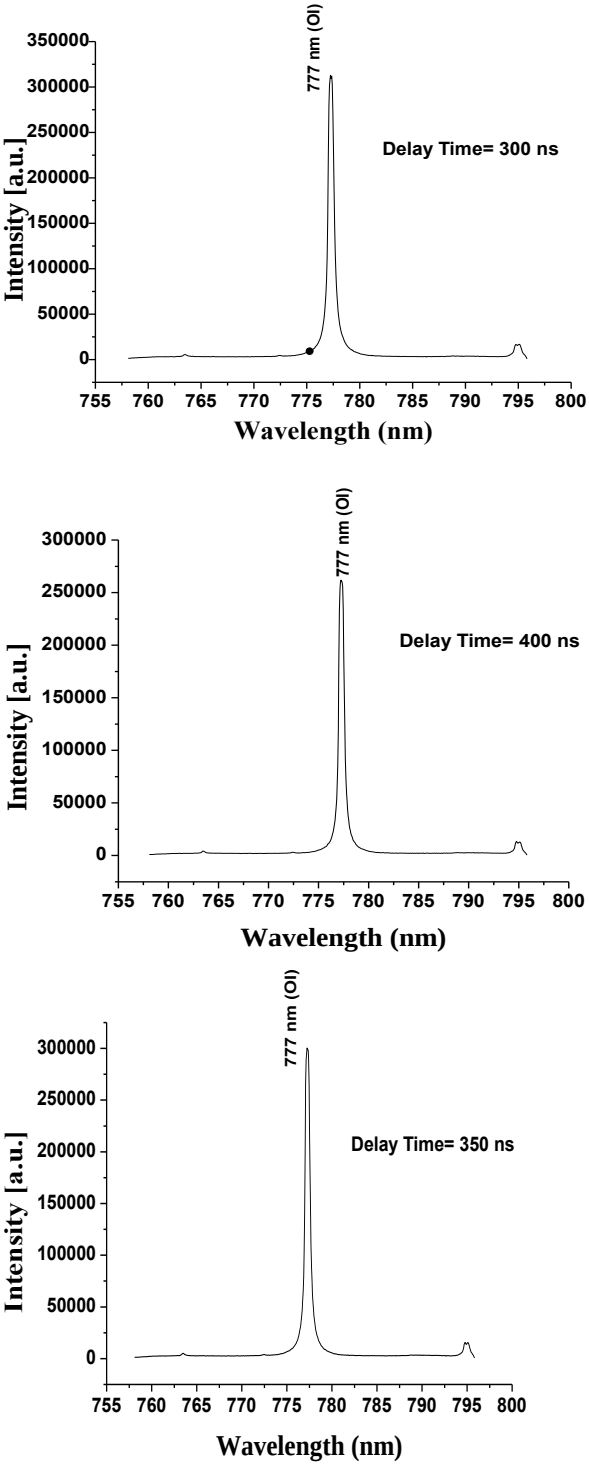

Fig. 2(a)-(c): Spectral emission lines of the neutral oxygen atom (OI) around 777 nm used for the determination of the lifetimes of the upper state at three different delay times t of (a) 300 ns, (b) 350 ns, (c) 400 ns.

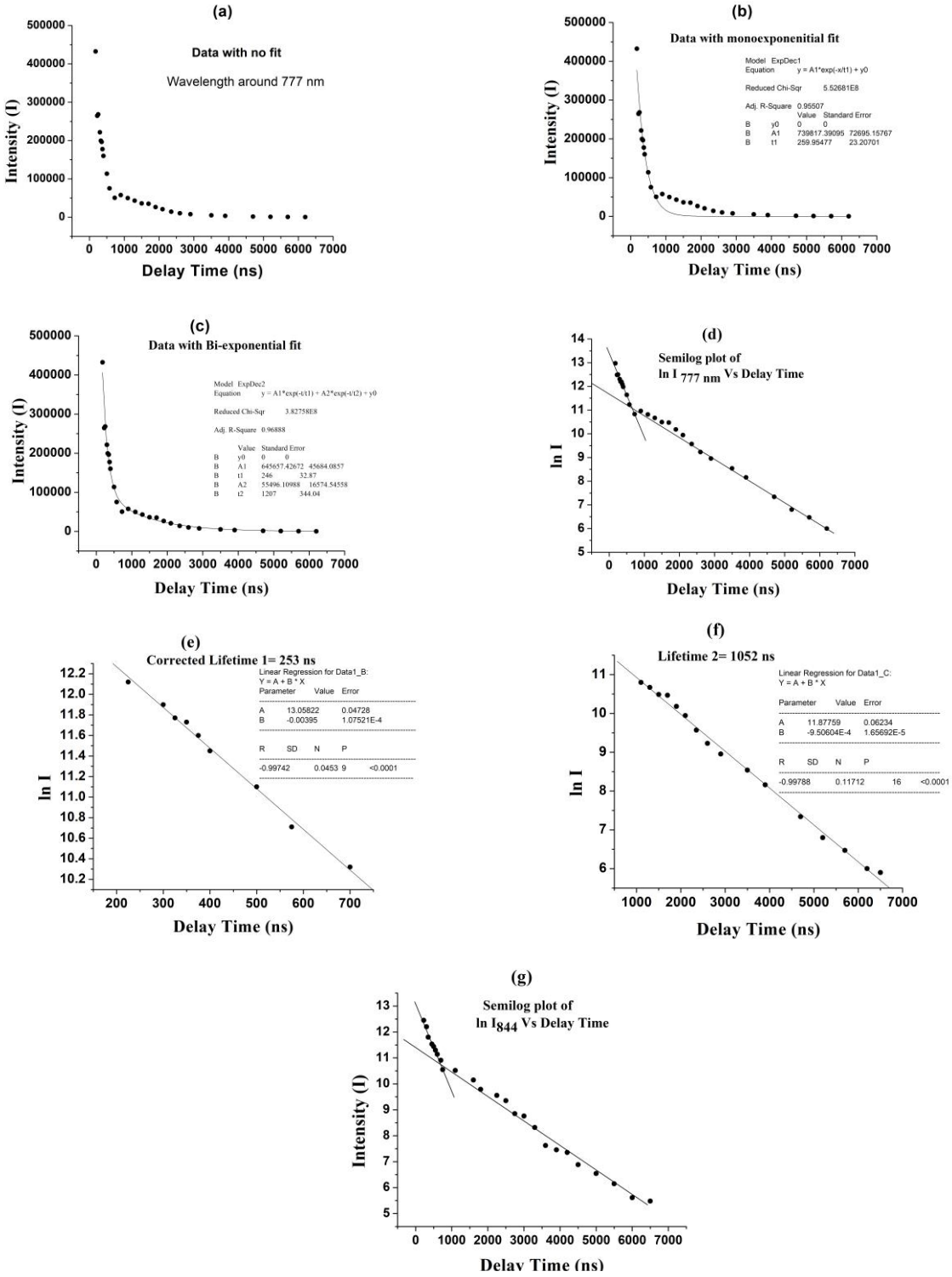

Fig. 3. Plot of the integrated intensity vs. delay time (in the range of 175-7000 ns) of the emission line of OI (at 777 nm) with (a) no fit, (b) mono-exponential fit ((R^2=0.95507)), and (c) bi-exponential (R^2=0.9688). Semi-logarithmic plots (i.e. ln I vs. delay time) of the OI emission line (at 777 nm) with linear fits in the range of (d) 175-6500 ns, (e) 175-700 ns (corrected), and (f) 900-6500 ns. (g) Semi logarithmic plot (ln I vs delay time) with linear fits in the range 175-6500 ns of the emission line around 844 nm.

The quicker decay process contains the contribution coming from the slower decay process, which is removed by subtraction. After this correction, the resulting semi-log plot for the delay range of 175-700 ns is obtained in Fig. 3(e), which has been drawn for OI atomic emission line at 777 nm. For this linear semi-log plot after the correction, the composite lifetime of three very closely spaced upper energy levels, $2s^2\ 2p^3\ (^4S^0)\ 3p\ ^5\mathbf{P_3}$ (777.194 nm), $2s^2\ 2p^3\ (^4S^0)\ 3p\ ^5\mathbf{P_2}$ (777.417nm) and $2s^2\ 2p^3\ (^4S^0)\ 3p\ ^5\mathbf{P_1}$ (777.539 nm), resulting to the transition to the $2s^2\ 2p^3\ (^4S^0)\ 3s\ ^5\mathbf{S_2}$ lower state (Fig. 4), were obtained as 253 ns. The results from the corrected semi-logarithmic plot (253 ns) match well with those obtained by the bi-exponential plot (241ns) (Table 1).

Table 1. Upper state lifetimes estimated for different transitions of OI around the wavelengths of 777 nm and 844 nm

Observed Lines (nm)	Transitions		By semi logarithmic fit			By bi-exponential fit	
	Upper state (Term value with J)	Lower state (Term value with J)	Spontaneous emission Lifetime (ns)		Plasma cooling temperature (excitation temperature) decay time (ns)	Spontaneous emission lifetime (ns)	Plasma cooling temperature (excitation temperature) decay time (ns)
			Uncorrected Value	Corrected Value			
777 (around)	$2s^2\ 2p^3\ (^4S^0)\ 3p\ ^5\mathbf{P_3}$ (777.194 nm) $2s^2\ 2p^3\ (^4S^0)\ 3p\ ^5\mathbf{P_2}$ (777.417 nm) $2s^2\ 2p^3\ (^4S^0)\ 3p\ ^5\mathbf{P_1}$ (777.539)	$2s^2\ 2p^3(^4S^0)\ 3s\ ^5\mathbf{S_2}$	263	253	1052	241	1207
844 (around)	$2s^2\ 2p^3\ (^4S^0)\ 3p\ ^3\mathbf{P_0}$ (844.625 nm) $2s^2\ 2p^3\ (^4S^0)\ 3p\ ^3\mathbf{P_2}$ (844.636 nm) $2S_2\ 2P_3\ (^4S^0)\ 3p\ ^3\mathbf{P_1}$ (844.676 nm)	$2s^2\ 2p^3(^4S^0)\ 3s\ ^3\mathbf{S_1}$	296	278	1136	271	1159

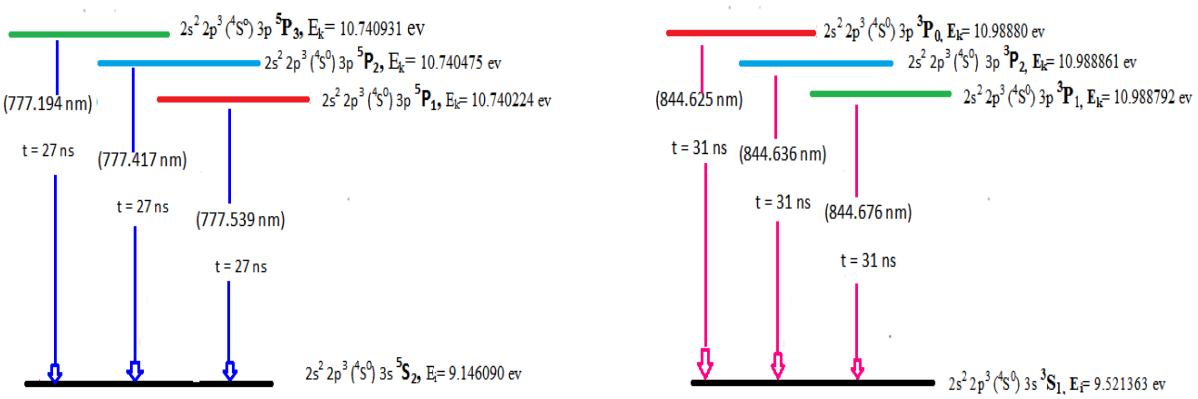

Fig. 4. Schematic diagram (drawn not to scale) of three upper states and associated lower state with relevant lifetimes.

The measured lifetimes in our experiment are much higher than the theoretical values of the lifetime for each transition between the energy levels in the case of 777 nm, which is 27 ns (Sansonetti and Martin 2005). This discrepancy might be linked primarily to the self-absorption between the energy levels where photons spontaneously emitted from the excited higher level of one atom can be absorbed by another atom of the same element in the lower state. In our previous work for determining the lifetime of the upper state of Nitrogen (Haider et al. 2014), three different transitions have three different lifetimes (67 ns, 104 ns, 198 ns), whereas, in this work, three lifetimes are very close (~27 ns). Unlike Nitrogen (Haider et al. 2014), emission lines result from the transitions from the three very closely spaced upper levels to the common lower level. As the emission lines are too close to be spectroscopically resolved, there should be considerable self-absorption for the proximity in energies of the three upper levels for the emission lines around 777 nm. The photon emitted from excited oxygen atoms/ions eventually decays to the ground state, emitting a photon and, after that, can be re-absorbed by another oxygen atom/ion with comparable energy spacing. The absorption-emission cycle can occur at very high rates (~few hundred MHz at room temperature) in a plasma plume temperature lifetime of the hot plasma. The magnitude of the decay constants for plasma cooling (excitation temperature) was measured as 1207 ns for wavelengths around 777 nm. For the OI line at 844 nm, the semi-logarithmic graphs (lnI vs. delay time) in Fig. 3(g) indicate the presence of two decay processes with characteristic slopes in two delay regions. The faster decay in the 175 ns to 800 ns interval of delay represents the lifetime of the higher state. In the case of around 844 nm line, for three upper levels $2s^2\ 2p^3\ (^4S^0)\ 3p\ ^3P_0$ [844.625 nm], $2s^2\ 2p^3\ (^4S^0)\ 3p\ ^3P_2$ (844.636nm) and $2s^2\ 2p^3\ (^4S^0)\ 3p\ ^3P_1$ (844.676 nm), the self-absorbed and radiation trapped lifetime (of the composite upper states) corresponding to the transition to $2s^2\ 2p^3\ (^4S^0)\ 3s\ \mathbf{^3S_1}$ common lower level (Fig. 4) was measured as 278 ns by the same procedure. The measured lifetime is much higher than the theoretical values of the lifetime (31 ns) (Sansonetti and Martin 2005). However, the magnitude of the decay constants for the plasma cooling was measured as 1159 ns for wavelengths around 844 nm, and the average decay constant for plasma cooling (1183 ns) matches well with the previously reported value (Cremers and Radziemski 1989).

Conclusions

In this study, we employed the well-known time-resolved LIBS (TR-LIBS) technique to simultaneously examine the lifetimes of the excited states of the neutral oxygen atom (OI) and the decay time of the laser-induced plasma temperature. The upper states of OI atom's lifetimes were measured by observing the atomic emission intensities as a function of the time interval between the laser's Q-switching and the ICCD's gate opening. The self-absorbed and radiation-trapped decay lifetimes of the excited OI atom for emission lines around the wavelengths of 777 nm and 844 nm are 253 ns and 278 ns, respectively, according to the outcomes from the corrected semi-logarithmic fit of the experimental data.

The measured lifetimes are much higher than the theoretical values (Sansonetti and Martin 2005) because of the self-absorption and radiation-trapping effect between the energy levels. Instead of departing the medium, a photon released spontaneously by one atom can be absorbed by another atom of the same element, resulting in the photon being trapped before it can escape and be detected. As a result, the self-absorption and the radiation trapping mechanism effectively 'delay' the photon's emission, resulting in an apparently much longer lifespan than the natural one.

The amount of time that elapses between the beginning of the laser plasma and the triggering of the laser pulse is significantly influenced by the energy of the laser pulse. Rather than the actual initiation time of the laser-induced plasma, the synchronous Q-switched laser pulse was responsible for the opening of the window of ICCD. Therefore,

shot-to-shot stability is crucial to ensure measurement accuracy, whereas error will be introduced if the laser pulse energy is not constant. Finally, within the limitations stated above, the method can be employed to measure the lifetimes of upper states (actual, self-absorbed, or radiation trapped) corresponding to different transitions of atoms and ions almost in any matrix. The technique works well for atomic emission lines in areas of the spectrum having a weak background originating from the plasma.

Conflicts of Interest

With regard to the publication of this paper, the authors have no conflicts of interest.

Acknowledgement

The experimental work was carried out in the Nonlinear Optics and Laser Spectroscopy Laboratory of the Center for Advanced Research in Sciences (CARS) of the University of Dhaka.

References

Aguilera J. and Aragón C. Multi-element Saha–Boltzmann and Boltzmann plots in laser-induced plasmas. *Spectrochimica Acta Part B: Atom. Spectro.* 2007; 62 (4): 378-385.

Balik S, Havey M, Sokolov I and Kupriyanov D. Optical pumping dynamics and near-resonance light scattering in an ultracold sample of R 87 b atoms. *Physical Review A* 2009; 79(3): 033418.

Berry H, Desesquelles J and Dufay M. Lifetime measurements of autoionizing levels by the beam-foil technique. *Physics Letters* 1971; *A* 36(3): 237-238.

Boldyrev S and Gwinn CR. Lévy model for interstellar scintillations. *Physical review letters* 2003; 91(13): 131101.

Camparo JC and MacKay R. Spectral mode changes in an alkali rf discharge. *J. Appl. Phys.* 2007; 101(5): 053303.

Cremers DA and Radziemski LJ. *Laser-induced plasmas and applications*: United States: Marcel Dekker Inc.1989.

Curtis LJ. Lifetime measurements. *Beam-Foil Spectroscopy* 1976; 63-109.

Hahn DW and Omenetto N. Laser-induced breakdown spectroscopy (LIBS), part I: review of basic diagnostics and plasma–particle interactions: still-challenging issues within the analytical plasma community. *Applied spectroscopy* 2010; 64(12): 335A-366A.

Haider AFMY and Khan Z. Determination of Ca content of coral skeleton by analyte additive method using the LIBS technique. *Optics & Laser Technology* 2012; 44(6): 1654-1659.

Haider AFMY, Ira MK, Khan Z and Abedin K. Radiative lifetime measurement of excited neutral nitrogen atoms by time resolved laser-induced breakdown spectroscopy. *J. Anal. Ato. Spectrom.* 2014; 29(8): 1385-1392.

Hannaford P and Lowe R. Determination of atomic lifetimes using laser-induced fluorescence from sputtered metal vapor. *Optical Engineering* 1983; 22(5): 532-544.

Hillenbrand G, Burnett K and Foot C. Effect of scattered radiation on sub-Doppler cooling. *Physical Review A* 1995; 52(6): 4763.

Hu M, Peng J, Niu S and Zeng H. Plasma-grating-induced breakdown spectroscopy. *Advanced Photonics* 2020; 2(6): 065001.

Hu M, Shi S, Yan M, Wu E and Zeng H. Femtosecond laser-induced breakdown spectroscopy by multidimensional plasma grating. *J. Anal. Ato. Spectrom.* 2022; 37(4): 841-848.

King G and Adams A. An accurate determination of the lifetime of the 63P state in mercury using a new electron-photon delayed coincidence apparatus. *J. Phys. B: Atom. Mol. Phys.* 1974; (1968-1987) 7(13): 1712.

Mayo R, Campos J, Ortiz M, Xu H, Svanberg S, Malcheva G and Blagoev K. Radiative lifetimes of Zr III excited levels. *The European Physical Journal D-Atomic, Molecular, Optical and Plasma Physics* 2006; 40(2): 169-173.

Mayo R, Ortiz M and Campos J. Experimental transition probabilities for lines arising from the 4d5p and 4d5d configurations of ZrIII. *J. Quant. Spectrosc. Radiat. Transf.* 2005; 94(1): 109-116.

Molisch AF and Oehry BP. *Radiation trapping in atomic vapours*: Oxford University Press 1998.

O'Brian T and Lawler J. Radiative lifetimes in BI using ultraviolet and vacuum-ultraviolet laser-induced fluorescence. *Astron. Astrophys.* 1992; 255: 420-426.

O'Brian T and Lawler J. Excited Level Lifetime Measurements. *Experimental Methods in the Physical Sciences*. United States: Academic Press, 1996; 217-254.

Pinnington E, Ansbacher W, Kernahan J, Ahmad T and Ge Z.-Q. Lifetime measurements for low-lying levels in Hg I and Hg II using the beam-foil technique. *Cana. J. Phys.* 1988; 66(11): 960-962.

Quintero M, Rodero A, Garcia M and Sola A. Determination of the excitation temperature in a nonthermodynamic-equilibrium high-pressure helium microwave plasma torch. *Appl. Spectrosc.* 1997; 51(6): 778-784.

Rajaraman K and Kushner MJ. A Monte Carlo simulation of radiation trapping in electrodeless gas discharge lamps. *J. Phys. D: Appli. Phys.* 2004; 37(13): 1780.

Sansonetti JE and Martin WC. *Handbook of Basic Atomic Spectroscopic Data*: American Institute of Physics 2005.

Shaikh NM, Rashid B, Hafeez S, Jamil Y and Baig M. Measurement of electron density and temperature of a laser-induced zinc plasma. *J. Phys. D: Appl. Phys.* 2006; 39(7): 1384.

Smith A, Read F and Imhof R. Measurement of the lifetimes of ionic excited states using the inelastic electron-photon delayed coincidence technique. *J. Phys. B: Atom. Mol. Phys.* 1975; (1968-1987) 8(17): 2869.

Stoita A, Vautey T, Jacquier B and S Guy. Impact of the radiation trapping on lifetime measurement of Er3+ doped glasses. *Journal of Lumin.* 2010; 130(7): 1119-1123.

Xu H, Persson A, Svanberg S, Blagoev K, Malcheva, G, Pentchev V, Biémont E, Campos J, Ortiz M and Mayo R. Radiative lifetime and transition probabilities in Cd I and Cd II. *Physical Review* 2004; *A* 70(4): 042508.

Yang Y, Zhigao L, Deshuo M and Mingjun M. Spectral characteristic of laser-induced plasma in soil. *Plasma Sci. Techno.* 2019; 22(1): 015502.

Zhang Q, Shang Q, Shi J, Chen J, Wang R, Mi Y, Du W, Shen C, Ma R and Qiu X. Wavelength tunable plasmonic lasers based on intrinsic self-absorption of gain material. *ACS Photonics* 2017; 4(11): 2789-2796.